



Effect of syringic acid and syringaldehyde on oxidative stress and inflammatory status in peripheral blood mononuclear cells from patients of myocardial infarction

Sumayya Shahzad¹ · Somaiya Mateen¹ · Tasneem Kausar² · Syed Shariq Naeem³ · Asif Hasan⁴ · Minhal Abidi¹ · Shahid M. Nayeem² · Abul Faiz Faizy¹ · Shagufta Moin¹

Received: 29 June 2019 / Accepted: 8 November 2019 / Published online: 10 December 2019
© Springer-Verlag GmbH Germany, part of Springer Nature 2019

Abstract

Oxidative stress and inflammation are considered as therapeutic targets in myocardial injury. The aim of the present study was to investigate the protective effect of syringic acid (SA) and syringaldehyde (SYD) on peripheral blood mononuclear cells (PBMCs) of myocardial infarction (MI) patients. PBMCs from MI patients were cultured in the presence and absence of SA and SYD. The level of tumor necrosis factor- α (TNF- α), interleukin-6 (IL-6), and nitric oxide (NO) was estimated. Reactive oxygen species (ROS) formation, oxidation of lipids, proteins, and activity of antioxidant enzymes were also quantified. To further determine biomolecular changes in treated PBMCs, Fourier transform infrared (FTIR) spectroscopic analysis was done. Molecular docking study was also conducted to evaluate the binding interaction of SA and SYD with various target proteins. SA and SYD treated PBMCs of MI patients showed decreased secretion of TNF- α , IL-6, and NO. Moreover, the content of ROS, level of lipid, and protein oxidation showed diminution by treatment with both the compounds. Enhanced antioxidant defense was also observed in treated PBMCs. The FTIR spectra of treated cells revealed safeguarding effect of SA and SYD on biomolecular structure. The molecular docking analysis displayed significant binding affinity of the two compounds towards TNF- α , IL-6, and antioxidant enzymes. Our findings demonstrated potent antioxidant and anti-inflammatory effects of SA and SYD on PBMCs of MI patients. Thus, SA and SYD supplementation might be beneficial in attenuating oxidative stress and inflammation in MI.

Keywords Myocardial infarction · PBMCs · Syringic acid · Syringaldehyde · Reactive oxygen species

Introduction

Myocardial infarction (MI) is a necrotic condition which is associated with various pathological alterations in myocardium (Li et al. 2012). Reactive oxygen species (ROS) are

produced excessively in cardiac tissue during MI, which directly react with cellular biomolecules like lipids, proteins, and DNA, instigating cell damage which at many times is irreversible leading to cell death (Kurian et al. 2016; Hensley et al. 2000). Chain reaction of lipid peroxidation mediated by ROS serves as the causative factor for deterioration of cell and organelle membrane. Furthermore, aldehydic breakdown products of lipid peroxidation as well as ROS react with cellular proteins and modify them. Hence, ROS hold the potential of directly impairing contractile function of cardiomyocytes by altering proteins that bring about excitation-contraction coupling. ROS also trigger endothelial dysfunction by oxidizing many cellular signaling proteins, which in turn mediate infiltration of inflammatory cells and thus, inflammation ensues. The common mediators of inflammation are cytokines like TNF- α , IL-6, IL-1 β , IFN- γ , and chemokines. Inflammatory mediators damage endothelium, promote local proteolysis, and plaque instability/rupture with subsequent formation of thrombus leading to myocardial

✉ Shagufta Moin
moinshagufta2@gmail.com

¹ Department of Biochemistry, Jawaharlal Nehru Medical College, Faculty of Medicine, Aligarh Muslim University, Aligarh, Uttar Pradesh, India
² Department of Chemistry, Faculty of Science, Aligarh Muslim University, Aligarh, Uttar Pradesh, India
³ Department of Pharmacology, Jawaharlal Nehru Medical College, Faculty of Medicine, Aligarh Muslim University, Aligarh, Uttar Pradesh, India
⁴ Centre of Cardiology, Jawaharlal Nehru Medical College, Faculty of Medicine, Aligarh Muslim University, Aligarh, Uttar Pradesh, India

ischemia (Sinisalo et al. 2000). The production of inflammatory cytokines correlated with clinical manifestations in MI (Kohsaka et al. 2005). Prolonged extension and over activation of inflammatory pathway in infarcted myocardium bring about many changes like cardiomyocytes loss, elevated tissue deterioration resulting in loss of ventricular wall integrity, expansion of fibrous tissue outside the initial infarct zone, and also systolic dysfunction of heart (Dobaczewski et al. 2010).

Association of MI with high morbidity and mortality is well known. Higher prevalence of MI lay down health and economic burden and demands further exploration of the disease and treatment strategies. There is mounting interest in finding phytochemicals of antioxidant nature that are capable of averting oxidative cellular and tissue injury during MI. Furthermore, plant-based drugs are economical and have less side effects.

Syringic acid (4-hydroxy-3,5-dimethoxybenzoic acid, SA) is a phenolic compound found in plants *Alpinia calcarata* Roscoe and *Morus nigra* L. SA possesses anti-microbial, anti-cancer, anti-inflammatory, and antioxidant properties (Güven et al. 2015; Kumar et al. 2012). SA was observed to normalize hyperglycemia in experimentally induced diabetes in rats through glycoprotein components and it also exhibited potent hepatoprotective efficacy by quenching free radicals in injured liver of mice (Muthukumaran et al. 2013). SA was also found to exert protection against osteoporosis as rats fed with SA showed enhanced femoral bone mineral density (Tanaka et al. 2017). Syringaldehyde (SYD) is found in *Manihot esculenta* and *Magnolia officinalis* plant species (Shen et al. 2009). SYD also has many beneficial properties like anti-microbial and anti-diabetic (Friedman et al. 2003; Huang et al. 2012). In human neutrophils, SYD showed inhibitory effect on formation of ROS and release of myeloperoxidase (Worm et al. 2001).

Herein, we explored the effect of exogenous supplementation of SA and SYD in cultured PBMCs of MI patients. We hypothesized that SA and SYD treatment of the patients PBMCs might protect them from oxidative and inflammatory injury.

Materials and methods

Chemicals

Syringic acid and syringaldehyde were obtained from Sigma-Aldrich, MO, USA. All chemicals used in this study were of analytical grade.

Patients and sampling

Twenty patients who were admitted to Coronary Care Unit (CCU) and diagnosed with MI were incorporated in this study.

Patients having age greater than 75 years, arrhythmia, serious conduction disturbances, and heart failure were not included. The study protocol was approved by the Institutional Ethics and Research Advisory Committee. Blood samples from patients were collected at the time of hospital admission. For comparison, blood samples were also collected from 20 age-matched healthy volunteers. All participants gave written informed consent prior to their enrolment.

Isolation of PBMCs

Blood was diluted with sterile phosphate-buffered saline (PBS) and layered over histopaque 1077 solution. The mixture was then centrifuged and the interphase layer of PBMCs was collected and washed with PBS. The isolated cells were suspended in PBS and counted by trypan blue exclusion assay. The cell viability was found to be > 95%.

MTT (3-(4,5-dimethylthiazol-2-yl)-2,5-diphenyltetrazolium bromide) assay

PBMCs from healthy individuals were suspended in RPMI-1640 (10% fetal bovine serum, 2mM L-glutamine streptomycin) medium and incubated with different concentrations of SA and SYD (5, 25, 50 and 100 μ M) for 24 h at 37 °C in 5% CO₂. After addition of MTT solution, cells were incubated for 3 h. Then the media was discarded and blue colored formazan crystals were solubilized with dimethyl sulfoxide (DMSO) and absorbance was recorded at 540 nm for determining cell viability (Mossmann 1983). Cells cultured without SA and SYD were used as control.

Experimental design

The PBMCs (1×10^6 cells/ml) in RPMI-1640 medium containing 10% fetal bovine serum (FBS), 2 mM solution of L-glutamine streptomycin were cultured for 24 h at 37 °C in CO₂ incubator humidified with 5% CO₂. The PBMCs were grouped and treated in the following way.

Control: PBMCs from healthy individuals serving as control.

MI: PBMCs from MI patients.

SA (5 μ M): PBMCs from MI patients treated with 5 μ M of SA.

SA (25 μ M): PBMCs from MI patients treated with 25 μ M of SA.

SA (50 μ M): PBMCs from MI patients treated with 50 μ M of SA.

SA (100 μ M): PBMCs from MI patients treated with 100 μ M of SA.

SYD (5 μ M): PBMCs from MI patients treated with 5 μ M of SYD.

SYD (25 μM): PBMCs from MI patients treated with 25 μM of SYD.

SYD (50 μM): PBMCs from MI patients treated with 50 μM of SYD.

SYD (100 μM): PBMCs from MI patients treated with 100 μM of SYD.

At the end of incubation period, the cells and supernatant were separated by centrifugation at 3000 rpm for 20 min. The culture supernatant was used for estimation of NO, TNF- α , and IL-6. The isolated cells were divided into two parts, one was used for estimation of ROS content and Fourier transform infrared (FTIR) analysis while the other part was lysed with lysing solution. The lysed cells were again centrifuged at 3000 rpm for 20 min at 4 °C to obtain supernatants for estimation of various biochemical parameters. The protein concentration of PBMCs was determined by following Lowry's method using BSA as standard (Lowry et al. 1951).

Measurement of NO

Griess reagent was used for determining the level of NO released by PBMCs in culture supernatant by following the method of Miranda et al. (Miranda et al. 2001).

Determination of ROS production

The cellular concentration of ROS was determined by dichloro dihydro fluorescein-diacetate ester (DCFH-DA) assay, according to the method of Keller et al. (Keller et al. 2004). The stained cells were also examined by confocal microscopy for capturing the representative images of each study group.

Assessment of malondialdehyde and protein carbonyl in PBMCs

For analysis of malondialdehyde (MDA) level in cell lysates, protocol described by Beuge and Aust was used (Beuge and Aust 1978), whereas concentration of protein carbonyl (PC) was quantitated by following the method of Reznick (Reznick and Packer 1994).

Measurement of GSH content

The amount of GSH in the lysate was estimated by following the protocol devised by Jollow et al. (Jollow et al. 1974).

Activity of antioxidant enzymes

The activity of superoxide dismutase (SOD) was assayed in the lysate according to the method of Marklund and Marklund (Marklund and Marklund 1974) and that of catalase by the method of Claiborne (Claiborne 1985). Estimation of glutathione peroxidase (GPx) activity in PBMCs was carried out by

following the protocol of Flohe and Gunzler (Flohe and Gunzler 1984).

Estimation of TNF- α and IL-6

ELISA kits were used for estimation of cell culture supernatant levels of TNF- α and IL-6 (Diacclone, France) according to the manufacturer's instructions. The lowest limits of detection was 8 pg/ml for TNF- α and 2 pg/ml for IL-6.

Fourier transform infrared spectroscopic analysis

The FTIR spectra for PBMCs of different groups of the study were taken on Perkin Elmer Spectrum Two FTIR spectrometer from wavenumber range of 1000–3000 cm^{-1} . The frequencies of the sharp bands of base line corrected spectra were also noted.

Molecular docking

The aim of molecular docking was to find the potential binding site of SA and SYD on TNF- α , IL-6, SOD, catalase, and GPx. We used Autodock 4.2 software for molecular docking using Lamarckian genetic algorithm (Morris et al. 2009). The three-dimensional structures of TNF- α , IL-6, SOD, catalase, and GPx were downloaded from Research Collaboratory for Structural Bioinformatics (RCSB) in the protein data bank (pdb) format with pdb ID 1TNF, 1IL6, 2C9V, 1QQW, and 2I3Y, respectively. Structure data format (SDF) of SA and SYD was obtained from ZINC data base. The ligand structures were minimized using steepest decent with 100 steps followed by conjugate gradient method by UCSF-chimera software (Morris et al. 1998). The minimized structure was saved in pdb format. During docking analysis, the macromolecules were fixed and ligands were allowed to explore in conformational space. The rest of the parameters used in docking was as described previously (Minhal Abidi et al. 2018). In each docking, 100 snapshots of complex were generated. The lowest energy conformation of the complex was selected as best docked conformation and further analyzed. UCSF-Chimera and LigPloyt⁺ (Laskowski and Swindells 2011) were used for post docking process and image generation.

Statistical analysis

Statistical analysis was carried out using Graph Pad Prism version 7.0 (CA, USA). Shapiro-Wilk's test was utilized for testing data normality. Differences among the study groups were determined by one-way ANOVA followed by post hoc Tukey's test for parametric variables and Kruskal Wallis test followed by Dunn's multiple comparison test for non-parametric variables. A probability level of $p < 0.05$ was considered as an indicator of statistical significance.

Results

Demographic and clinical characteristics

Age and body mass index (BMI) of MI patients did not exhibit significant difference, whereas admission blood glucose and systolic blood pressure were significantly elevated in the patients than control group. In addition, lipid profile of the patient group was also found to be altered as compared to healthy individuals ($p < 0.05$) (Table 1).

Effect of SA and SYD on viability of cells

PBMCs were incubated with varied concentration of SA and SYD (5, 25, 50, and 100 μM) for 24 h and the viability of cells was assessed by MTT assay. We detected no significant change in cell viability at all the concentrations of SA with respect to control set. Similarly, viability of PBMCs was not observed to be altered at 5, 25, and 50 μM of SYD treatment as compared to cell viability in the absence of the compounds in control cells. However, cell viability at 100 μM of SYD treatment was found to decrease significantly than control PBMCs (Fig. 1).

Effect of SA and SYD on production of NO

The amount of NO in cell-free supernatants of the patients was significantly higher than control samples. However, upon treatment of MI patients PBMCs with SA at 5, 25, 50, and 100 μM concentration, released NO content in supernatants goes on decreasing. Among all these concentrations of SA, maximum inhibitory effect on NO production was found at dose of 50 μM . Similarly, incubation of PBMCs of MI

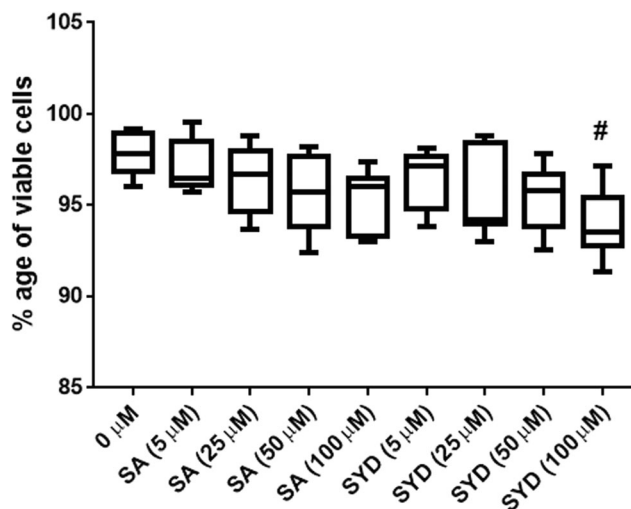


Fig. 1 Effect of treatment with different concentration of SA and SYD on viability of PBMCs. Each box plot indicates interquartile range, horizontal line indicates median value, lower whisker represents minimum value, and upper whisker represents maximum value. Results are from three independent experiments done in triplicate. # $p < 0.05$ versus control set (0 μM) analyzed by one-way ANOVA followed by post hoc Tukey's test

patients with SYD reduced the formation of NO in dose dependent manner with maximum beneficial effect at concentration of 50 μM (Fig. 2). This implied that both SA and SYD limited the production of NO in PBMCs, dose dependently. Thus, 5, 25, and 50 μM concentrations of SA and SYD were used in the following experiments.

Effect of SA and SYD on ROS level

ROS are considered as key players that persuade oxidative stress. In the present study, level of ROS in cultured

Table 1 Demographic and clinical characteristics of the study subjects

Variables	Healthy controls ($n = 20$)	MI patients ($n = 20$)
Age	48.65 \pm 10.09	50.8 \pm 9.02
Sex (M/F)	18/2	17/3
Body mass index (kg/m)	24.59 \pm 2.26	25.11 \pm 3.64
Hypertension	–	3
Diabetes mellitus	–	2
Hyperlipidemia	–	3
Smoking	–	1
Blood glucose (mg/dl)	97.35 \pm 14.59	125.1 \pm 27.63*
Systolic blood pressure (mm Hg)	127.6 \pm 20.56	150.8 \pm 19.76*
Diastolic blood pressure (mm Hg)	82.35 \pm 13.60	85.2 \pm 11.97
Total cholesterol (mg/dl)	156.37 \pm 20.33	192.72 \pm 23.49*
Triglycerides (mg/dl)	123.15 \pm 22.46	142.58 \pm 24.57*
HDL cholesterol (mg/dl)	46.11 \pm 9.32	37.02 \pm 10.24*
LDL cholesterol (mg/dl)	85.62 \pm 23.74	127.18 \pm 26.57*

Values are expressed as mean \pm SD. * $p \leq 0.05$ vs healthy controls

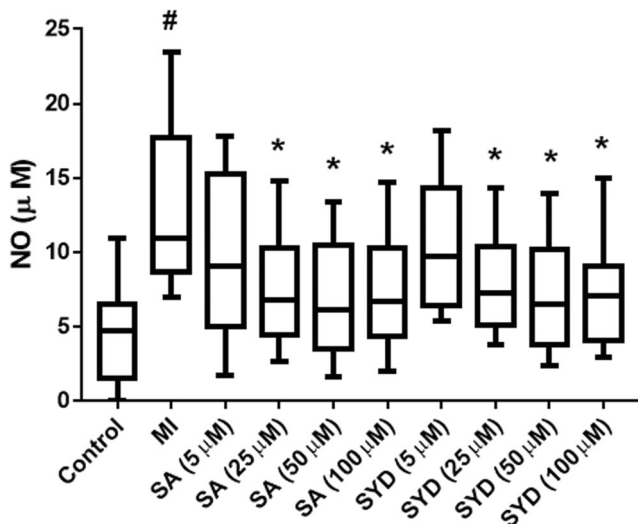


Fig. 2 PBMCs of MI patients produced higher NO than controls. However, SA and SYD treatment resulted in decreased NO production. Each box plot indicates interquartile range, horizontal line indicates median value, lower whisker represents minimum value, and upper whisker represents maximum value. *n* = 20 in each group; #*p* < 0.05 versus control group, **p* < 0.05 versus MI group analyzed by one-way ANOVA followed by post hoc Tukey's test

PBMCs of MI patients was highly elevated as compared to cultured PBMCs of healthy individuals. The cells incubated with SA and SYD demonstrated less production of ROS and this decrease in ROS level was found to be in proportion to the concentration of SA and SYD. So, SA- and SYD-treated PBMCs resulted in inhibition of ROS formation (Fig. 3).

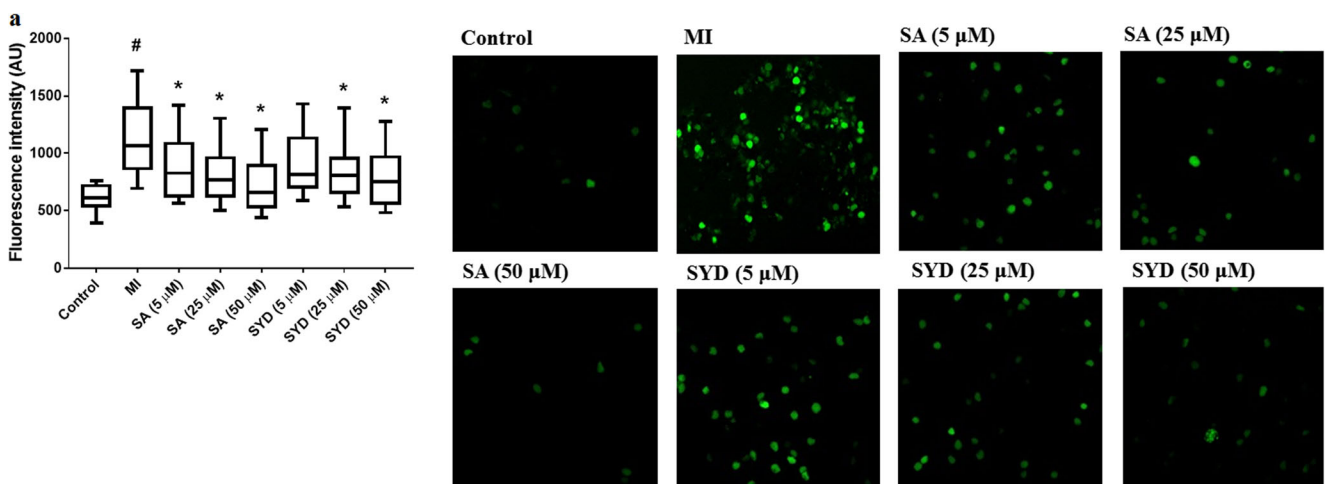


Fig. 3 a Enhanced ROS formation was found in MI patient PBMCs which decreased upon treatment with SA and SYD. Photomicrographs showing generation of ROS in different groups of the study. Each box plot indicates interquartile range, horizontal line indicates median value,

Protective effect of SA and SYD on lipid peroxidation and protein carbonylation

Malondialdehyde (MDA) which is a biochemical marker of oxidative lipid damage was found to be significantly higher in cell lysates of MI patients than that in control volunteers. In case of cells of MI patients incubated with SA and SYD, MDA content reduced dose dependently with least level at 50 μM of SA and SYD. Protein carbonyls (PC), the end product of ROS-induced protein oxidation is known to impair protein function; its level was highest in MI group indicating elevated level of protein oxidation in MI patients. However, PC content decreased upon treatment of cells with SA and SYD in concentration dependent fashion (Fig. 4a, b).

Beneficial effect of SA and SYD on enzymatic and non-enzymatic antioxidants

The intracellular concentration of non-enzymatic antioxidant, reduced glutathione (GSH) was observed to be highly depleted in MI patients than control group. Also, the activity of different antioxidant enzymes, namely, SOD, catalase, and GPx, was significantly diminished in PBMCs of MI patients as compared to control cells. Interestingly, in SA and SYD treatment groups, the depletion in enzymatic and non-enzymatic antioxidants was not as profound as observed in MI group. That is, incubation of patient PBMCs with SA and SYD resulted in increased GSH content and elevated activities of the antioxidant enzymes in dose-dependent manner (Fig. 5a–d).

lower whisker represents minimum value, and upper whisker represents maximum value. *n* = 20 in each group; #*p* < 0.05 versus control group, **p* < 0.05 versus MI group analyzed by one-way ANOVA followed by post hoc Tukey's test

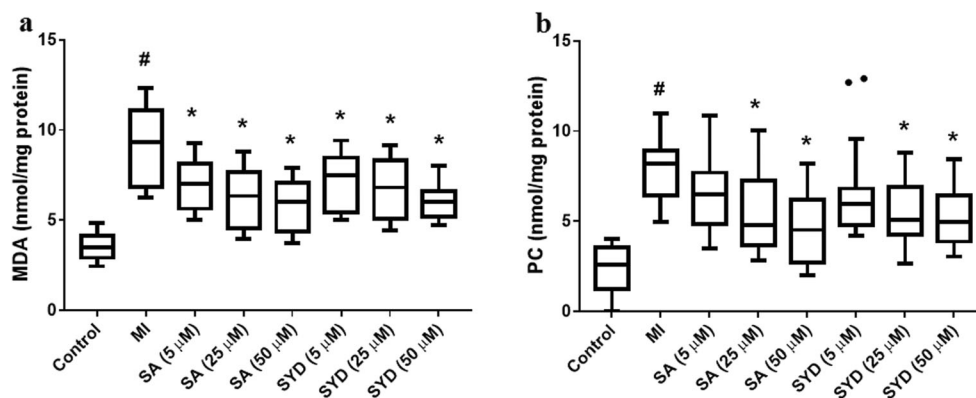


Fig. 4 Attenuating effect of SA and SYD supplementation on MDA (a) and PC (b) levels in PBMCs. Each box plot indicates interquartile range, horizontal line indicates median value, lower whisker represents minimum value, and upper whisker represents maximum value. Circles

represent outliers. $n = 20$ in each group; # $p < 0.05$ versus control group, * $p < 0.05$ versus MI group analyzed by one-way ANOVA followed by post hoc Tukey's test for MDA and Kruskal-Wallis test followed by Dunn's multiple comparison test for PC

SA and SYD inhibited cellular production of TNF- α and IL-6

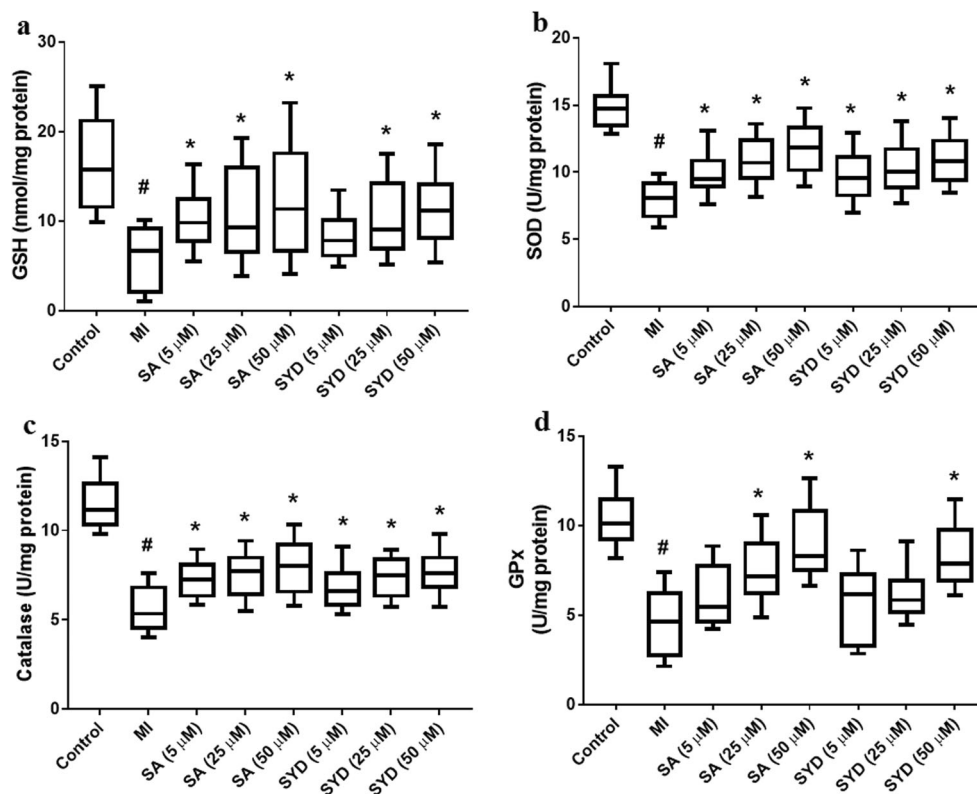
To determine the effect of SA and SYD supplementation on inflammatory status of patient PBMCs, we estimated the culture supernatant level of TNF- α and IL-6. We found significantly higher concentration of the two pro-inflammatory cytokines in culture supernatant of MI patients than that of control group. On the other hand, SA and SYD treatment of cells

diminished the secretion of TNF- α and IL-6 in concentration dependent way (Fig. 6a, b).

Effect of SA and SYD on biochemical changes in PBMCs

The infrared spectra of biological system arise due to the vibrational modes of different molecular functional groups present in the biological system. The infrared spectrum of cells

Fig. 5 Effect of incubation with SA and SYD on cellular concentration of GSH (a) and activity of antioxidant enzymes SOD (b), catalase (c), GPx (d). Each box plot indicates interquartile range, horizontal line indicates median value, lower whisker represents minimum value, and upper whisker represents maximum value. $n = 20$ in each group; # $p < 0.05$ versus control group, * $p < 0.05$ versus MI group analyzed by one-way ANOVA followed by post hoc Tukey's test



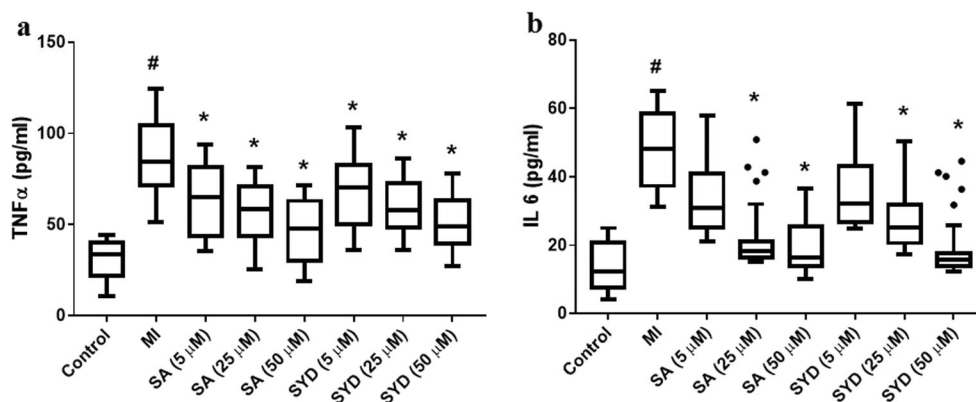


Fig. 6 Effect of SA and SYD on secretion of cytokines, TNF- α (a) and IL-6 (b) by PBMCs. Each box plot indicates interquartile range, horizontal line indicates median value, lower whisker represents minimum value, and upper whisker represents maximum value. Circles represent outliers.

$n = 20$ in each group; # $p < 0.05$ versus control group, * $p < 0.05$ versus MI group analyzed by one-way ANOVA followed by post hoc Tukey's test for TNF- α and Kruskal-Wallis test followed by Dunn's multiple comparison test for IL-6

and tissues is constituted by absorption bands that are similar to those found in the infrared spectrum of a mixture of proteins, carbohydrates, DNA, and lipids. The spectral analysis of PBMCs was performed in three distinct wave number ranges, namely 1000–1300 cm^{-1} , 1500–1700 cm^{-1} , 2800–3000 cm^{-1} . These wave number regions correspond to DNA, protein, and lipids, respectively. Also, prior studies performed FTIR analysis of PBMCs in these wave number regions to evaluate the effect of phytochemicals on cellular biomolecular alterations (Kiruthiga et al. 2010; Mateen et al. 2019). As shown in Fig. 7, the spectra of control group consist of two absorbance bands at 1646 cm^{-1} and 1547 cm^{-1} , corresponding to amide I and amide II which convey information about the secondary structure of proteins. Amide I band arises as a result of C=O stretching vibrations and Amide II band corresponds to C–N stretching, NH and CH₂ bending modes. The absorption intensity of the spectra of MI group in 1500–1700 cm^{-1} region decreased as compared to control group indicating the occurrence of perturbations in structure or content of proteins. Shift in the position of amide bands was also seen in spectra of MI group from that in control group. However, cells of MI patients incubated with SA and SYD showed increase in absorbance of amide I band nearer to that of control spectra (Fig. 7a).

The spectral bands located in the region 2800 and 3000 cm^{-1} arise as a result of CH stretching in CH₃ and CH₂ groups mainly of endogenous lipids. Control group showed two peaks at 2854 cm^{-1} and 2931 cm^{-1} corresponding to stretch vibrations of the methylene group. But the spectra of MI group showed decreased absorbance and shift in peak positions as compared to control group, which might be due to enhanced peroxidative damage to membrane lipids in PBMCs of MI patients. But, when cells of MI patients were incubated with SA and SYD, the spectral absorbance showed increment, probably due to inhibition of lipid peroxidation (Fig. 7b).

The bands observed in spectral region 1000 to 1300 cm^{-1} are due to stretching modes of nucleic acids mainly, with slight contributions from phospholipids. In Fig. 7c, it can be seen that spectra of control group showed bands at 1035 cm^{-1} , 1096 cm^{-1} , and 1217 cm^{-1} corresponding to skeletal trans conformation of C–C bond in DNA, symmetric and asymmetric stretching of phosphate, respectively. The spectra of MI group showed distinctive features than control group. However, incubation of PBMCs with SA and SYD tends to inhibit the alterations in DNA of the cells as signified by decreased FTIR absorption and amelioration of peak positions in SA- and SYD-treated groups (Fig. 7c). The shift in positions of bands in different biomolecules are given in Table 2.

Binding interaction analysis of SA and SYD

Recently, molecular docking emerges as an attractive tool to predict the binding geometry of ligand molecules at the active site of target macromolecules (protein or DNA) in a non-covalent fashion. It reveals the interaction details of ligand and macromolecule such as hydrogen bond (H-bond), hydrophobic interaction, and binding energy. We performed molecular docking to check the binding efficacy of SA and SYD with pro-inflammatory cytokines and antioxidant enzymes SOD, catalase, and GPx. The docking energy, number of H-bonds, and hydrophobic residues of different proteins that interact with SA/SYD are listed in Table 3. The binding pose of SA/SYD with target proteins is illustrated in Figs. 8, 9, 10, and 11 as 3D and 2D representations.

Inflammatory cytokines like TNF- α , IL-1 β , and IL-6 are involved in induction of intense aseptic inflammatory response causing fibrosis like damage to the myocardium during MI. TNF- α was found to form complex with SA via three H-bonds with residues Gln61B, Pro117C, Tyr119B having binding free energy of -4.58 kcal/mol. Moreover, the binding pattern of SA and TNF- α revealed that SA penetrates deeper

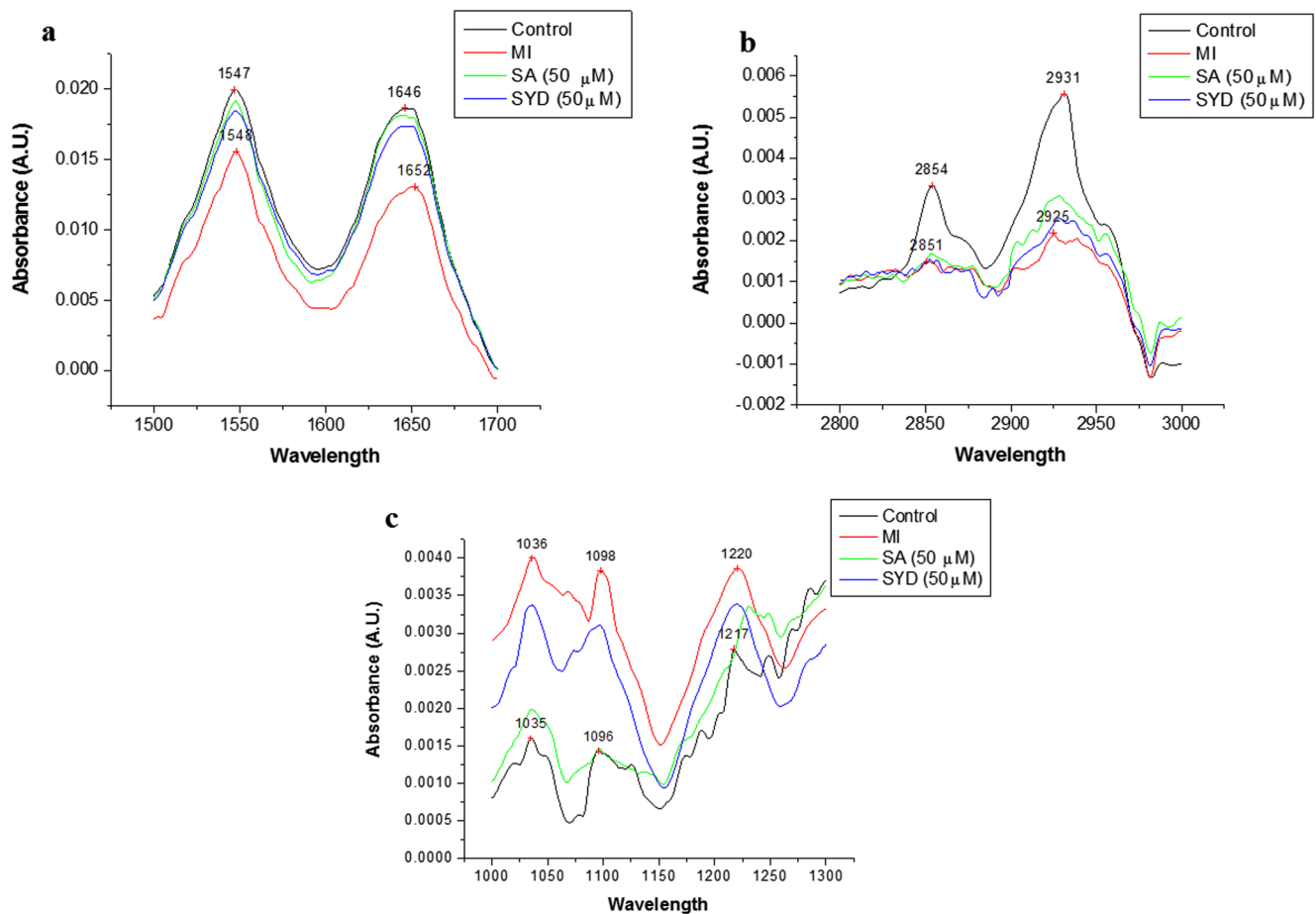


Fig. 7 FTIR absorption spectra of PBMCs obtained from healthy controls, MI patients with and without treatment with SA and SYD in the regions, 1500–1700 cm^{-1} (a), 2800–3000 cm^{-1} (b), and 1000–

1300 cm^{-1} (c) corresponding to proteins, lipids, and DNA, respectively. The absorbance peaks in control and MI groups are marked

inside the trimeric interface of TNF- α . The binding affinity of SA and IL-6 was found to be slightly less than that of SA-TNF- α complex as binding energy of SA-IL-6 complex was -3.76 kcal/mol. Also, the interaction of SA with IL-6 showed two H-bonds formation by Arg41 and Lys172 residues (Fig. 8). The docking complex of SYD and TNF- α displayed similar hydrogen bonding interaction but released relatively higher energy (-4.66 kcal/mol) than that of SA-TNF- α complex and SYD formed three H-bonds with Gln61B, Pro117C, and Tyr119C residues of TNF- α . Furthermore, the complex of SYD and IL-6, by releasing -3.14 kcal/mol of free energy,

leads to the formation of three H-bonds involving Thr44, Glu107, and Ser108 residues (Fig. 9). The binding analysis of SA/SYD to TNF- α and IL-6, in light of ELISA results indicate that SA and SYD may have inhibitory effect on these proteins and the two ligands could function as biotherapeutics for abrogating the excessive production of these pro-inflammatory cytokines.

SOD and catalase are vital antioxidant enzymes that scavenge free radicals; these enzymes carry out scavenging of superoxide radical and hydrogen peroxide (H_2O_2) before their interaction to form more reactive hydroxyl radical. GPx

Table 2 Absorption bands of proteins, lipids, and DNA in control, MI, and treated PBMCs from FTIR spectral analysis

Groups	Amide I cm^{-1}	Amide II cm^{-1}	Lipids cm^{-1}	DNA cm^{-1}
Control	1646	1547	2854	2931
MI	1652	1548	2851	2925
SA (50 μM)	1645	1548	2853	2928
SYD (50 μM)	1650	1548	2852	2929

Table 3 Binding energy, hydrogen bonds, and hydrophobic interactions formed between the ligands and target proteins

Ligand	Target protein	Binding energy (kcal/mol)	No. of H-bonds	H-bonded amino acid residues	Key residues of hydrophobic interaction
SA	TNF α	-4.58	3	Gln 61B, Pro 117C, Tyr 119B	Ala 96A, Pro 117 A, Pro 117 B, Ile 118A, Ile 118B, Ile 118 C, Tyr 119 A, Tyr 119 C
	IL 6	-3.76	2	Arg 41, Lys 172	Lys 42, Cys 45, Asn 46, Glu 52
	SOD	-4.44	2	Lys 9, Val 148	Val 7, Asn 53, Cys 146, Gly 147
	Catalase	-3.46	2	His 305, Lys 306	Pro 151, Val 302, Pro 304, Gln 442
	GPx	-3.43	2	Lys 167, His 200	Thr 165, Ser 168, Trp 181
SYD	TNF α	-4.66	3	Gln 61B, Pro 117C, Tyr 119C	Pro 117A, Pro 117 B, Ile 118 A, Ile 118B, Ile 118C, Tyr 119A, Tyr 119B
	IL 6	-3.14	3	Thr 44, Glu 107, Ser 108	Glu 43, Arg 105, Phe 106
	SOD	-3.11	3	His 63, His 80, Lys 136	Pro 62, Arg 69, Lys 70, Thr 137
	Catalase	-4.15	2	Ala 345	Ile 42, Gln 53, Lys 221, Glu 344, Glu 420, His 421, Val 429, Tyr 425
	GPx	-3.03	2	Arg 197	Pro 157, His 158, Pro 159, Met 196

quenches lipid hydroperoxides (LOOH) and H_2O_2 utilizing GSH. That is SOD, catalase and GPx serve as the first line of cellular defense against oxidative injury. From molecular docking studies, SA was observed to have much stronger affinity towards SOD (-4.44 kcal/mol) followed by catalase (-3.46 kcal/mol) and GPx (-3.43 kcal/mol), whereas SYD interacted with greater affinity to catalase

(-4.15 kcal/mol) followed by SOD (-3.11 kcal/mol) and GPx (-3.03 kcal/mol). Two H-bonds were found to form between Lys9 and Val148 of SOD with O5 and O3 atoms of SA, having H-bond distance of 2.83 Å and 2.87 Å respectively. In SA-catalase complex, two H-bonds were formed with residues His305 and Lys306 involving the common atom O4 of SA. In SA-GPx complex, two H-

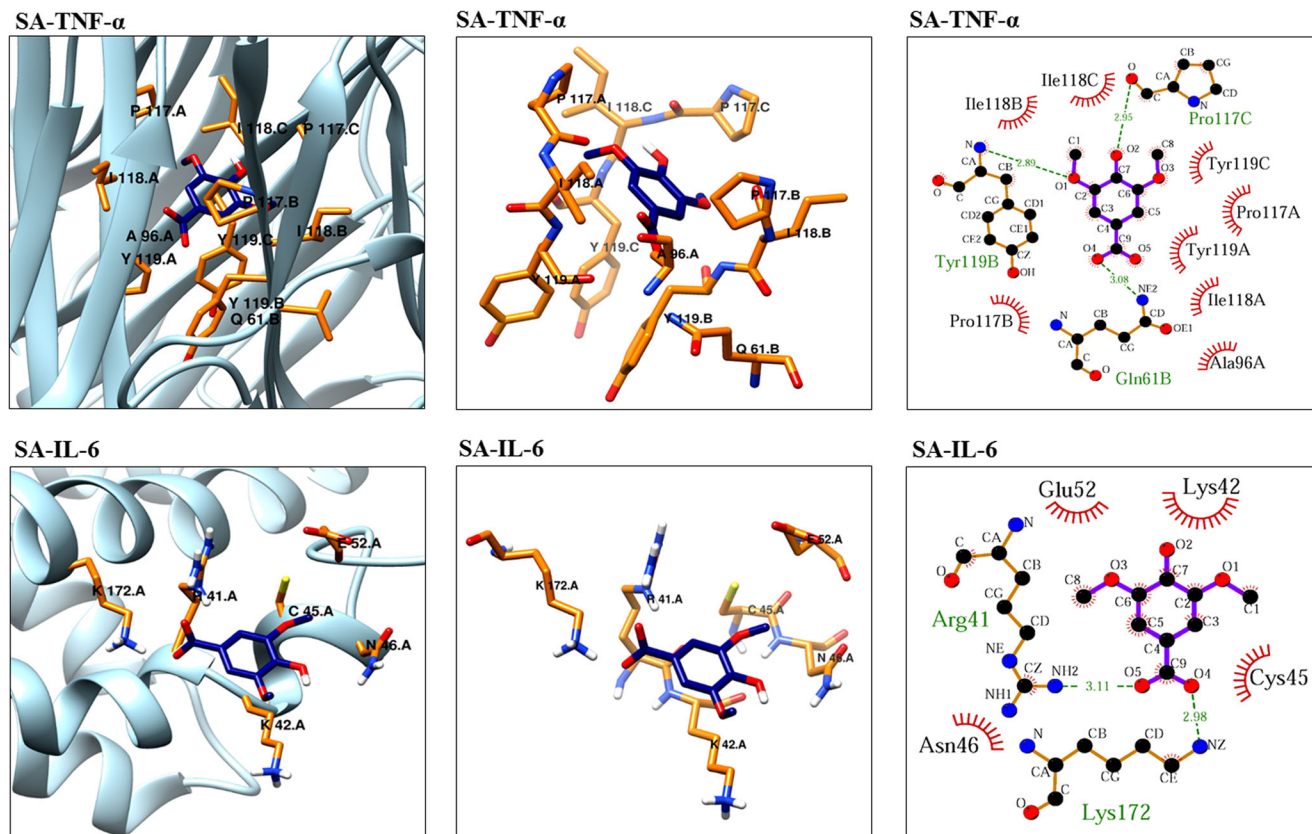


Fig. 8 Binding mode of SA with TNF- and IL-6. The green colored dotted lines are hydrogen bonding interactions while orange colored curves signify hydrophobic interactions

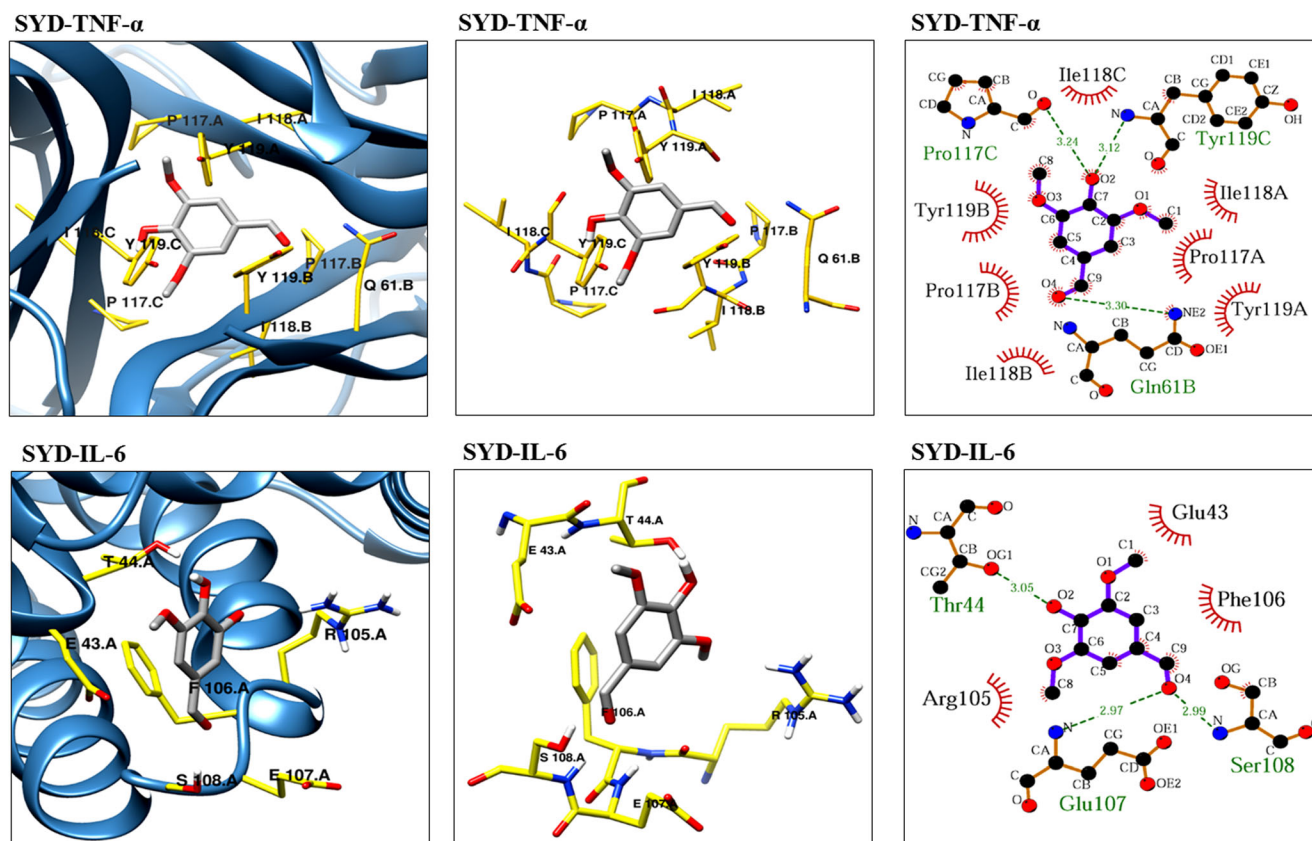


Fig. 9 Molecular docking interactions of SYD with TNF- α and IL-6. The green colored dotted lines are hydrogen bonding interactions while orange colored curves signify hydrophobic interactions

bonds were formed with Lys167 and His200 residues of the enzyme (Fig. 10). SYD was observed to form three H-bonds with His63, His80, and Lys136 residues of SOD. In addition, the complexes of catalase and GPx enzyme with SYD showed bidentate H-bond formation with Ala345 of catalase and Arg197 of GPx (Fig. 11). From in vitro study, we found increase in antioxidant enzyme activity in cells of MI patients upon their incubation with SA and SYD as compared to the untreated patient PBMCs. These results along with the findings of docking analysis indicate that binding of SA and SYD to the antioxidant enzymes might be enhancing their antioxidant activity.

Discussion

In the current study, we observed accelerated generation of NO and ROS by PBMCs of MI patients indicating that enlarged production of oxidant species occurs in MI. The increased secretion of NO by the cells might be due to stimulation of inducible nitric oxide synthase (iNOS) as iNOS mediated excessive NO production was found in experimental animal model of MI (Sithuraj and Viswanadha 2018). Moreover, iNOS-mediated excessive formation of NO is linked with suppressed myocardial contractility and NO reacts with

superoxide radicals to form peroxynitrite which damage proteins and thus further cause cell damage (Wollert and Drexler 2002). When patient cells were incubated with SA and SYD, the level of ROS and NO declined, owing to their scavenging by both the compounds.

In addition, MDA content was also raised in cells of MI patients because of ROS instigated damage of membrane lipids. The peroxidation of lipids makes the cells more prone to oxidative damage (Sithuraj and Viswanadha 2018). Similarly, PC level was augmented in cell lysate of MI patients pointing towards enhanced oxidative impairment of proteins which in turn cause structural and functional alterations in proteins. Previous studies have also reported elevated plasma level of MDA and PC in MI patients than healthy controls (Musthafa et al. 2017; Shahzad et al. 2018). The amount of both biomarkers diminished upon incubation of cells with SA and SYD in dose dependent manner, implying that SA and SYD defended against deteriorating membranous lipids and formation of toxic carbonyl compounds.

GSH, the cellular thiol plays a major role in bio-reduction, detoxification, and conjugation reactions. The antioxidant enzymes SOD and catalase protect cells from oxidative damage. SOD dismutates superoxide radical and catalase decomposes H_2O_2 (Rajadurai and Stanely Mainzen Prince 2006). GSH also serves as a substrate for GPx, glutathione-S-transferase,

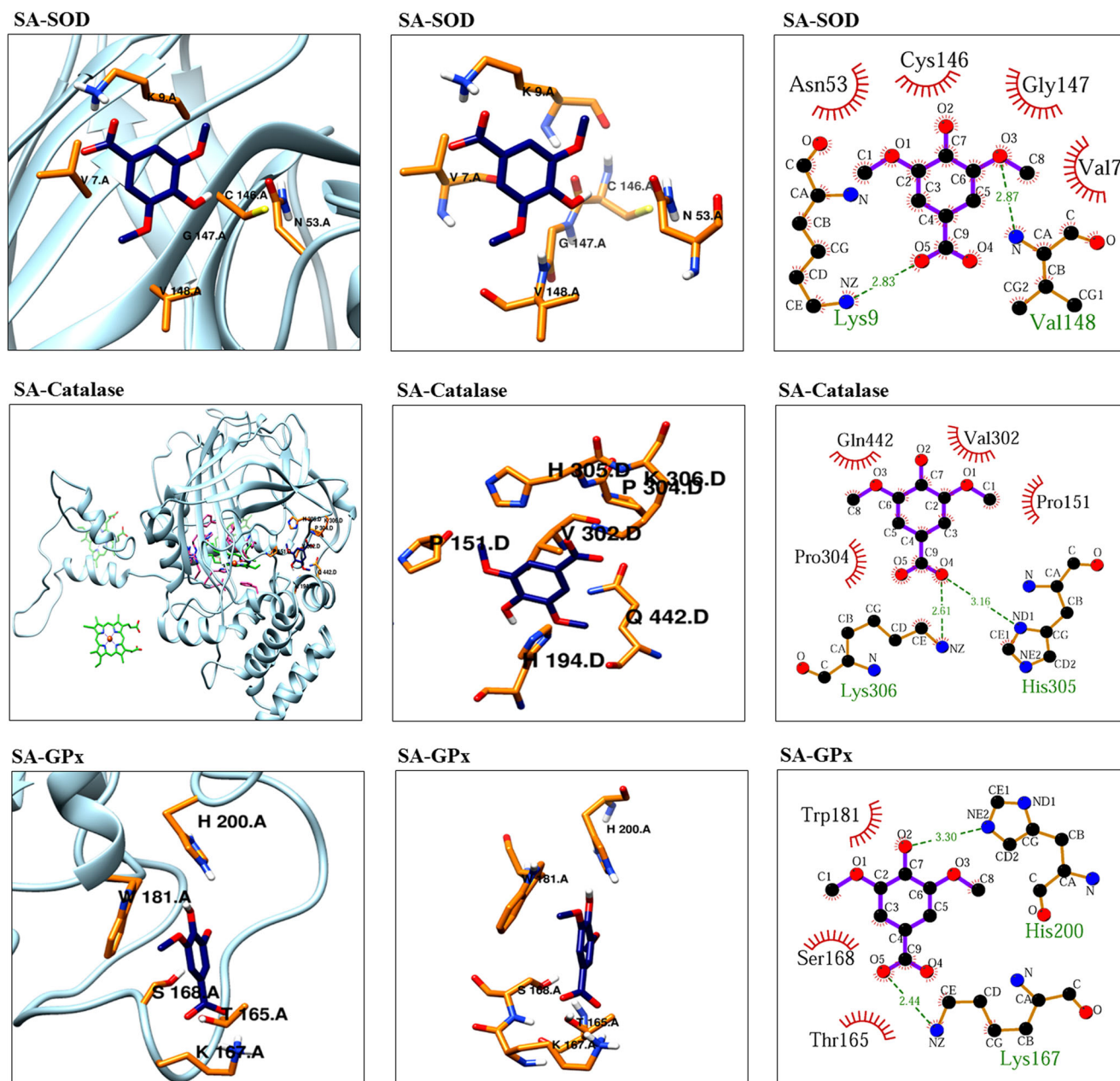


Fig. 10 Molecular structures representing binding of SA with SOD, catalase, and GPx. The green colored dotted lines are hydrogen bonding interactions while orange colored curves signify hydrophobic interactions

and some other enzymes, associated with scavenging of free radicals. GPx eliminates stable peroxides from biological system. Our results are in line with the earlier study which reported significantly decreased levels of GSH and antioxidant enzymes in CAD patients than controls (Musthafa et al. 2017). The significant reduction in amount of cellular GSH and antioxidant enzymes in MI group than control might be due to their increased utilization in combating overly produced ROS and RNS or direct inactivation of enzymes by ROS. The elevated level of GSH and activity of antioxidant enzymes in SA and SYD treated groups showed that the compounds quench the intracellularly produced ROS in MI patients PBMCs. This

could be due to either less utilization of cellular antioxidants in presence of exogenously supplemented SA/SYD or prevention of free radicals mediated inactivation of the antioxidant enzymes. Thus, SA and SYD protected cellular antioxidant defense system from oxidative deterioration in MI patients.

Pro-inflammatory cytokines such as TNF- α and IL-6 set up a deleterious cascade of events that results in contractile dysfunctionality of heart by mediating oxidative stress, endothelial dysfunction, induction of myocyte hypertrophy, and apoptosis (Hedayat et al. 2010). Eskandari et al. reported high expression of TNF- α and IL-6 in PBMCs of congestive heart failure (CHF) patients than healthy controls (Eskandari et al.

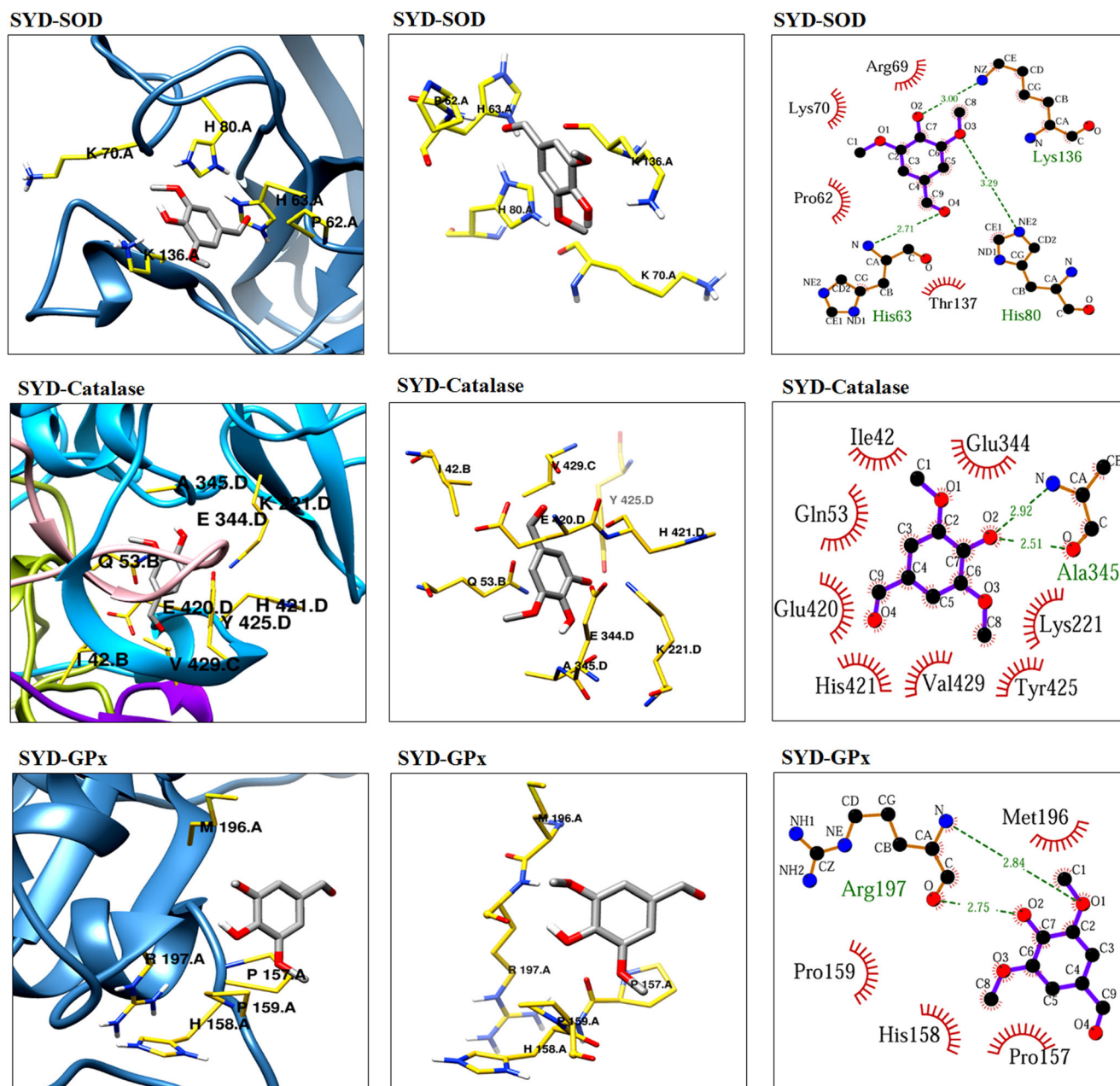


Fig. 11 Molecular docking conformation of SYD with SOD, catalase, and GPx. The green colored dotted lines are hydrogen bonding interactions while orange colored curves signify hydrophobic interactions

2018). Also, serum level of TNF- α , IL-1 β , and IL-6 was found to be highly raised in MI patients than control group (Shahzad et al. 2019). In consistent with the above findings, we noticed significantly higher secretion of TNF- α and IL-6 by cultured PBMCs of MI patients. The patients' cells incubated with SA and SYD showed dose-dependent diminution in secretion of both the cytokines. Decrease in TNF- α concentration might had led to reduced activation of NF- κ B pathway which mediates inflammation, as NF- κ B pathway is responsible for induction of numerous inflammatory genes like IL-1 β , IL-6, TNF- α , and cyclooxygenase-2 (Liu et al. 2017). Thus, SA and SYD possess anti-

inflammatory activity as they suppressed the PBMC secretion of TNF- α and IL-6.

The FTIR analysis of PBMCs further supported the oxidative damage to proteins, lipids, and DNA molecules of the cells in MI patients. It is known that, FTIR spectroscopy is utilized to determine vibrational modes of the functional groups of biomolecules and it is sensitive to conformation and structure of molecules. Hence, it is used for exploration of biochemical changes in these molecules (Gao et al. 2000). The shifting of amide bands towards decreased absorbance in MI group than control group, indicates secondary structural alterations in proteins. Thus, these results reflected the altered

cellular protein profile in MI patients. Upon treatment of patients' cells with SA and SYD, the spectral absorbance increased. This showed that SA and SYD treatment protected the membrane proteins, probably because of their antioxidant potential. In addition, we found alterations in the methylene stretching IR bands of the lipid hydrocarbon chains in patients' cells with respect to controls; this shift in absorbance of CH₂ stretching is indicator of peroxidation of membranous lipids and disruption of membrane fluidity (Zelig et al. 2011). The FTIR spectra of PBMCs incubated with SA and SYD showed increased absorption by lipid molecules than that in MI group, signifying that the compounds prevented alteration in lipid profile of PBMCs. Similarly, alterations in spectral bands corresponding to symmetric and asymmetric stretching of phosphate in DNA were found in patient cells than in controlled set. The possible reasons for the augmented absorption of DNA in MI group may be modifications like perturbations in the functional groups of DNA. However, the absorption spectra of DNA was decreased and thus, DNA damage when the cells were incubated with SA and SYD.

Docking analysis is an important tool for evaluating targets for different ligands. Through such studies interaction between a protein and a small molecule at the atomic scale can be established (Balamurugan et al. 2012). The structure of SA and SYD allowed their binding with many targets and thus, they may serve as antagonist or agonist to the bound protein. The images of docked structures revealed that SA and SYD snugly fit into the active site of many target proteins with the release of free energy. Furthermore, good binding interaction was noted between SA/SYD and pro-inflammatory cytokines (TNF- α and IL-6). Since, we found decrement in released TNF- α and IL-6 in SA- and SYD-treated patients PBMCs, the binding interaction of SA and SYD with TNF- α /IL-6 may account for the inhibitory effect of SA and SYD on TNF- α /IL-6 secretion. These findings could be underlying reason for decrease in level of TNF- α and IL-6 in cultured cells of MI patients incubated with SA and SYD than untreated PBMC culture. In silico results of interaction of SA and SYD also indicated their binding to SOD, catalase, and GPx. As we found enhancement in the activity of these enzymes in treated cells of MI patients with respect to untreated cells, binding of SA and SYD to the antioxidant enzymes might be adding up their antioxidant action.

Conclusion

Our study showed reduction in ROS content, inflammation, oxidative, and structural biomolecular alterations, whereas GSH level and function of antioxidant enzymes were enhanced upon SA and SYD treatment of PBMCs from MI patients. So, therapeutics consisting of SA and SYD may alleviate oxidative and inflammatory injury in MI patients. The

current study provides some of the experimental basis for development of therapeutic strategies including SA and SYD for patients of MI. However, clinical assessment is needed to validate the usage of SA and SYD in humans.

Acknowledgments The authors extend their sincere appreciation to the research facility provided by Chairperson, Department of Biochemistry, Department of Physiology, Jawaharlal Nehru Medical College and University Sophisticated Instrumentation Centre, Aligarh Muslim University.

Authors contribution statement SS, S Moin, SM: conceived and designed research. SS: conducted experiments. TK, AH, SSN, MA, AFF: contributed new reagents and analytical tools. SS, S Moin, TK, SMN: analyzed data. SS: wrote the manuscript. All authors read and approved the manuscript.

Compliance with ethical standards The study protocol was approved by the Institutional Ethics and Research Advisory Committee.

Conflict of interest The authors declare that they have no competing interests.

References

- Li H, Xie YH, Yang Q, Wang SW, Zhang BL, Wang JB, Cao W, Bi LL, Sun JY, Miao S, Hu J, Zhou XX, Qiu PC (2012) Cardioprotective effect of paeonol and danshensu combination on isoproterenol-induced myocardial injury in rats. *PLoS One* 7:e48872
- Kurian GA, Rajagopal R, Vedantham S, Rajesh M (2016) The role of oxidative stress in myocardial ischemia and reperfusion injury and remodeling: revisited. *Oxidative Med Cell Longev* 2016
- Hensley K, Robinson KA, Gabbita SP, Salsman S, Floyd RA (2000) Reactive oxygen species, cell signaling, and cell injury. *Free Radic Biol Med* 28:1456–1462
- Sinisalo J, Paronen J, Mattila KJ, Syrjälä M, Alftan G, Palosuo T, Nieminen MS, Vaarala O (2000) Relation of inflammation to vascular function in patients with coronary heart disease. *Atherosclerosis* 149:403–411
- Kohsaka S, Menon V, Lowe AM, Lange M, Dzavik V, Sleeper LA, Hochman JS, SHOCK Investigators (2005) Systemic inflammatory response syndrome after acute myocardial infarction complicated by cardiogenic shock. *Arch Intern Med* 165:1643–1650
- Dobaczewski M, Xia Y, Bujak M, Gonzalez-Quesada C, Frangogiannis NG. CCR5 signaling suppresses inflammation and reduces adverse remodeling of the infarcted heart, mediating recruitment of regulatory T cells. *Am J Pathol* 2010; 176:2177–2187. [PubMed: 20382703]
- Güven M, Aras AB, Topaloğlu N, Özkan A, Şen HM, Kalkan Y, Okuyucu A, Akbal A, Gökmen F, Coşar M (2015) The protective effect of syringic acid on ischemia injury in rat brain. *Turk J Med Sci* 45:233–240
- Kumar S, Prahalathan P, Raja B (2012) Syringic acid ameliorates (L)-NAME-induced hypertension by reducing oxidative stress. *Naunyn Schmiedeberg's Arch Pharmacol* 385:1175–1184
- Muthukumar J, Srinivasan S, Venkatesan RS, Ramachandran V, Muruganathan U (2013) Syringic acid, a novel natural phenolic acid, normalizes hyperglycemia with special reference to glycoprotein components in experimental diabetic rats. *Journal of Acute Disease* 2(4):304–309

- Tanaka T, Kawaguchi N, Zaima N, Moriyama T, Fukuta Y, Shirasaka N (2017) Antiosteoporotic activity of a syringic acid diet in ovariectomized mice. *J Nat Med* 71(4):632–641
- Shen CC, Ni CL, Shen YC, Huang YL, Kuo CH, Wu TS, Chen CC (2009) Phenolic constituents from the stem bark of *Magnolia officinalis*. *J Nat Prod* 72:168–171
- Friedman M, Henika PR, Mandrell RE (2003) Antibacterial activities of phenolic benzaldehydes and benzoic acids against *Campylobacter jejuni*, *Escherichia coli*, *Listeria monocytogenes*, and *Salmonella enterica*. *J Food Prot* 10:1811–1821
- Huang CH, Chen MF, Chung HH, Cheng JT (2012) Antihyperglycemic effect of syringaldehyde in streptozotocin-induced diabetic rats. *J Nat Prod* 75:1465–1468
- Worm E, Beukelman CJ, Berg AJJ, Kroes BH, Labadie RP, Dijk H (2001) Effects of methoxylation of apocynin and analogs on the inhibition of reactive oxygen species production by stimulating human neutrophils. *Eur J Pharmacol* 433:225–230
- Mossman T (1983) Rapid colorimetric assay for cellular growth and survival: application to proliferation and cytotoxicity assays. *J Immunol Methods* 65:55–63
- Lowry OH, Rosebrough NJ, Farr AL, Randall RJ (1951) Protein measurement with the Folin phenol reagent. *J Biol Chem* 193:265–275
- Miranda KM, Espey MG, Wink DA (2001) A rapid, simple spectrophotometric method for simultaneous detection of nitrate and nitrite. *Nitric Oxide* 5:62–71
- Keller A, Mohamed A, Drose S, Brandt U, Fleming I, Brandes RP (2004) Analysis of dichloro dihydro fluorescein and dihydro calcein as probes for the detection of intracellular reactive oxygen species. *Free Radic Res* 38(12):1257–1267
- Buege JA, Aust SD (1978) [30] Microsomal lipid peroxidation. *Methods Enzymol* 52: 302–310
- Reznick AZ, Packer L (1994) [38] Oxidative damage to proteins: spectrophotometric method for carbonyl assay. *Methods Enzymol* 233: 357–363
- Jollow D, Mitchell J, Na Z, Gillette J (1974) Bromobenzene-induced liver necrosis. Protective role of glutathione and evidence for 3, 4-bromobenzene oxide as the hepatotoxic metabolite. *Pharmacology* 11:151–169
- Marklund S, Marklund G (1974) Involvement of the superoxide anion radical in the autoxidation of pyrogallol and a convenient assay for superoxide dismutase. *Eur J Biochem* 47:469–474
- Claiborne A. Catalase activity, *Handbook of methods for oxygen radical research*, ed Greenwald R.A. (CRC Press, Boca Raton, FL). 1985
- Flohé L, Günzler WA (1984) [12] Assays of glutathione peroxidase. *Methods Enzymol* 105: 114–120
- Morris GM, Huey R, Linstrom W, Sanner MF, Belew RK, Goodsell DD, Olson AJ (2009) Valence bond theory for chemical dynamics. *J Comput Chem* 30:2785–2791
- Morris GM, Goodsell DS, Halliday RS, Huey R, Hart WE, Belew RK, Olson AJ (1998) Design, synthesis and evaluation of genistein-polyamine conjugates as multi-functional anti-Alzheimer agents. *J Comput Chem* 19:1639–1662
- Minhal Abidi M, Khan S, Ahmad S, Kausar T, Nayeem SM, Islam S, Ali A, Alam K, Moinuddin (2018) Biophysical and biochemical studies on glycoxidatively modified human low density lipoprotein. *Archives of Biochemistry and Biophysics* 645:87–99
- Laskowski RA, Swindells MB (2011) LigPlot+: multiple ligand–protein interaction diagrams for drug discovery. *J Chem Inf Model* 51: 2778–2786
- Kiruthiga PV, Pandian SK, Devi KP (2010) Silymarin protects PBMC against B (a) P induced toxicity by replenishing redox status and modulating glutathione metabolizing enzymes—an in vitro study. *Toxicol Appl Pharmacol* 247(2):116–128
- Mateen S, Rehman MT, Shahzad S, Naeem SS, Faizy AF, Khan AQ, Khan MS, Husain FM, Moin S (2019) Anti-oxidant and anti-inflammatory effects of cinnamaldehyde and eugenol on mononuclear cells of rheumatoid arthritis patients. *Eur J Pharmacol* 852:14–24
- Sithuraj S, Viswanadha VP. Berbamine protects the heart from isoproterenol induced myocardial infarction by modulating eNOS and iNOS expressions in rats. *Journal of Applied Biomedicine*. 2018 Jun 7
- Wollert KC, Drexler H (2002) Regulation of cardiac remodeling by nitric oxide, focus on cardiac myocyte hypertrophy and apoptosis. *Heart Fail Rev* 7:317–325
- Musthafa QA, Abdul Shukor MF, Ismail NA, Mohd Ghazi A, Mohd Ali R, IF MN, Dimon MZ, Wan Ngah WZ (2017) Oxidative status and reduced glutathione levels in premature coronary artery disease and coronary artery disease. *Free Radic Res* 51(9–10):787–798
- Shahzad S, Hasan A, Faizy AF, Mateen S, Fatima N, Moin S (2018) Elevated DNA damage, oxidative stress and impaired response defense system inflicted in patients with myocardial infarction. *Clin Appl Thromb Hemost* 24:780–789
- Rajadurai M, Stanely Mainzen Prince P (2006) Preventive effect of naringin on lipids, lipoproteins and lipid metabolic enzymes in isoproterenol-induced myocardial infarction in wistar rats. *J Biochem Mol Toxic* 20:191–197
- Hedayat M, Mahmoudi MJ, Rose NR, Rezaei N (2010) Pro-inflammatory cytokines in heart failure: double-edged swords. *Heart Fail Rev* 15(6):543–562
- Eskandari V, Amirzargar AA, Mahmoudi MJ, Rahnemoon Z, Rahmani F, Sadati S, Rahmati Z, Gorzin F, Hedayat M, Rezaei N. Gene expression and levels of IL-6 and TNF α in PBMCs correlate with severity and functional class in patients with chronic heart failure. *Irish Journal of Medical Science* (1971-). 2018; 187(2):359–68
- Shahzad S, Mateen S, Hasan A, Moin S (2019) GRACE score of myocardial infarction patients correlates with oxidative stress index, hsCRP and inflammation. *Immunobiology*. 224(3):433–439
- Liu T, Zhang L, Joo D, Sun SC (2017) NF- κ B signaling in inflammation. *Signal transduction and targeted therapy* 2:17023
- Gao T, Ci Y, Jian H, An C. FTIR investigation of the interaction of tumor cells treated with caffeic acid and chlorogenic acid. *Vibrational spectroscopy*. 2000; 24 (2):225–31. OOR Kiruthiga PV, Pandian SK, Devi KP
- Zelig U, Mordechai S, Shubinsky G, Sahu RK, Huleihel M, Leibovitz E, Nathan I, Kapelushnik J. Pre-screening and follow-up of childhood acute leukemia using biochemical infrared analysis of peripheral blood mononuclear cells. *Biochimica et Biophysica Acta (BBA)-General Subjects*. 2011 Sep 1; 1810(9):827–35
- Balamurugan R, Stalin A, Ignacimuthu S (2012) Molecular docking of γ -sitosterol with some targets related to diabetes. *Eur J Med Chem* 47: 38–43

Publisher's note Springer Nature remains neutral with regard to jurisdictional claims in published maps and institutional affiliations.